0021-972X/04/$15.00/0
Printed in U.S.A.

The Journal of Clinical Endocrinology & Metabolism 89(1):392–399

doi: 10.1210/jc.2003-030682

Genetic and Structural Evaluation of Fatty Acid Transport Protein-4 in Relation to Markers of the Insulin Resistance Syndrome

K. GERTOW, M. BELLANDA, P. ERIKSSON, S. BOQUIST, A. HAMSTEN, M. SUNNERHAGEN, AND R. M. FISHER

Department of Medicine (K.G., P.E., S.B., A.H., R.M.F.), Atherosclerosis Research Unit, King Gustaf V Research Institute, and Department of Medical Biochemistry and Biophysics (M.S.), Karolinska Institutet, S-171 76 Stockholm, Sweden; and Department of Organic Chemistry (M.B.), University of Padova, 35131 Padova, Italy

Disturbances in fatty acid metabolism are involved in the etiology of insulin resistance and the related dyslipidemia, hypertension, and procoagulant state. The fatty acid transport proteins (FATPs) are implicated in facilitated cellular uptake of nonesterified fatty acids (NEFAs), thus potentially regulating NEFA concentrations and metabolism. The aim of this study was to investigate polymorphic loci in the FATP4 gene with respect to associations with fasting and postprandial lipid and lipoprotein variables and markers of insulin resistance in 608 healthy, middle-aged Swedish men and to evaluate possible mechanisms behind any associations observed.

Heterozygotes for a Gly209Ser polymorphism (Ser allele frequency 0.05) had significantly lower body mass index and, correcting for body mass index, significantly lower triglyceride concentrations, systolic blood pressure, insulin concentrations, and homeostasis model assessment index compared with common homozygotes. A three-dimensional model of the FATP4 protein based on structural and functional similarity with adenylate-forming enzymes revealed that the variable residue 209 is exposed in a region potentially involved in protein-protein interactions. Furthermore, the model indicated functional regions with respect to NEFA transport and acyl-coenzyme A synthase activity and membrane association.

These findings propose FATP4 as a candidate gene for the insulin resistance syndrome and provide a structural basis for understanding FATP function in NEFA transport and metabolism. (*J Clin Endocrinol Metab* 89: 392–399, 2004)

INCREASED CONCENTRATIONS OF plasma nonesterified fatty acids (NEFAs) are one of the hallmarks of obesity and insulin resistance (reviewed in Ref. 1), as are increased fasting and postprandial triglyceridemia, low high-density lipoprotein (HDL) cholesterol concentrations, and increased formation of small, dense low-density lipoprotein (LDL) particles along with hypertension and a procoagulant state. Cellular fatty acid (FA) uptake is believed to be facilitated by a number of membrane-associated proteins, including plasma membrane FA binding protein (FABP pm) (2), FA translocase (FAT/CD36) (3), and FA transport proteins (FATPs) (4). The importance of facilitated transmembrane FA transport in both lipid and carbohydrate metabolism have been demonstrated in animal models (5, 6).

FATP4 belongs to a highly homologous and evolutionary conserved gene family with six members (FATP1–6) in man, each with a distinct expression pattern (7). FATP4 expression is most prominent in central nervous tissue, intermediate in intestine, heart, liver, and pancreas, is relatively low in skeletal muscle, and has been observed in adipose tissue (8). The human FATP4 gene consists of 12 coding exons spanning more than 17 kb of genomic DNA on chromosome 9q34, giving rise to a 71-kDa protein, containing an AMP-binding motif (also called phosphate-binding loop or p-loop) conserved in FATP1–6, acyl-coenzyme A (acyl-CoA) synthases and other members of the adenylate-forming enzyme superfamily (9, 10). The AMP-binding motif has been suggested to convey acyl-CoA synthase activity to FATPs and homologous proteins (9, 11, 12) as part of their proposed role in NEFA metabolism. The importance of FATP4 function in long-chain fatty acid uptake by enterocytes, in which FATP4 is the most abundant FATP, has been demonstrated *in vitro* (13).

We have previously shown that the rare allele of an intronic polymorphism in the FATP1 gene was associated with increased postprandial triglyceridemia and a shift toward a smaller, more dense LDL phenotype (14). The aims of this study were to investigate variation within the FATP4 gene with respect to associations with fasting and postprandial lipid and lipoprotein variables and markers of insulin resistance in healthy, middle-aged Swedish men and to evaluate possible mechanisms behind any associations observed.

Subjects and Methods

Subjects

A total of 608 50-yr-old men living in the county of Stockholm were selected at random from a registry of permanent residents (15). Exclusion criteria were non-Caucasian descent, chronic disease, history of

Abbreviations: acyl-CoA, Acyl-coenzyme A; apo, apolipoprotein; BMI, body mass index; FA, fatty acid; FACS, fatty acyl-CoA synthase; FATP, fatty acid transport protein; HDL, high-density lipoprotein; HOMA, homeostasis model assessment; LDL, low-density lipoprotein; NEFA, nonesterified fatty acid; OFTT, oral fat tolerance test; SBP, systolic blood pressure; seACS, *Salmonella enterica* acetyl-CoA synthase; S_f, Svedberg floatation rate; SNP, single-nucleotide polymorphism; TG, triglyceride; VLDL, very low-density lipoprotein.

cardiovascular disease, familial hypercholesterolemia, alcohol abuse, psychiatric disorders, and participation in other ongoing studies. Samples were collected after an overnight fast. Studies were approved by the Karolinska Hospital local ethics committee, and all subjects gave their informed consent.

Oral fat tolerance test

A subset of 105 consecutive individuals from the cohort with the apolipoprotein (apo) E3/E3 genotype underwent an oral fat tolerance test (OFTT) of the mixed-meal type (total energy content, 1000 kcal; 60% energy from fat) (15). Blood samples were drawn before and up to 6 h after food intake.

Biochemical analyses

Triglyceride (TG) and cholesterol concentrations in plasma and major lipoproteins were determined enzymatically (15). Very low-density lipoprotein (VLDL), LDL, and HDL were isolated from fasting plasma by a combination of preparative ultracentrifugation and precipitation of apoB-containing lipoproteins (15). Fasting and postprandial TG-rich lipoproteins; Svedberg floatation rate [$S_f > 400$; S_f 60–400; and S_f 20–60] were subfractionated by cumulative density ultracentrifugation (15). ApoB48 and apoB100 concentrations in isolated lipoprotein subfractions were determined by SDS-PAGE, staining with Coomassie G-250, and subsequent scanning (15). Blood glucose, plasma NEFA, insulin, and proinsulin concentrations were measured with standard methods (15).

Sequencing

PCR was used to amplify regions surrounding reported single-nucleotide polymorphisms (SNPs) in the FATP4 gene, namely a C/T polymorphism at position −856 of the putative proximal promoter region, a G/A polymorphism at position 625 in exon 3 (Gly209Ser), a C/T polymorphism at position 1542 in exon 10, and a G/A polymorphism at position 149 of intron 11. For the proximal promoter region, the primers 5′-CCTGGATGTCAGAAGAGTGAACTG-3′ and 5′-TGCTGGTAGAGAACATGAGGTCTG-3′ were used in 1.5 mM $MgCl_2$ with 2 U AmpliTaq Gold (Applied Biosystems, Piscataway, NJ). Hot-start touch-down thermocycling was performed with 25 final cycles of 94 C for 45 sec, 53 C for 30 sec, and 72 C for 90 sec. For the exon 3 fragment, the primers 5′-GTGAGGTCCATGCCAGCCTG-3′ and 5′-CACCTGTGAAGCCCTTGTCAG-3′ were used in 2.0 mM $MgCl_2$ with 1 U of AmpliTaq Gold. Hot-start touch-down thermocycling was performed with 25 final cycles of 30-sec steps at 94 C, 56 C, and 72 C. For the exon 10 C/T and intron 11 G/A polymorphisms, the primers 5′-GACGCAGGGTACACCTGGTGACAG-3′ and 5′-CCTTGTCCTAGGCCAGCCTCTCTC-3′ were used in 1.5 mM $MgCl_2$ with 2 U Taq DNA polymerase (Promega, Madison, WI) using touch-down thermocycling with 30 final cycles of 94 C for 30 sec, 56 C for 30 sec, and 72 C for 60 sec. Purified PCR products were sequenced with the primers 5′-CCAGACTTCGCTCGTTCTCGCATG-3′, 5′-TTGTCAGGGCAACTGGGAAG-3′, 5′-CCTTGTGGTCAAACAAATCCTTGG-3′, and 5′-GCTCAGGTCTTGGAGAAGGAACTG-3′ for the proximal promoter, exon 3, exon 10, and intron 11 polymorphisms, respectively, using the DYEnamic ET terminator cycle sequencing premix kit (Amersham Pharmacia Biotech, Piscataway, NJ). Sequencing reactions were run on an ABI 377 automated DNA sequencer and the results analyzed with the ABI Prism software (Amersham Pharmacia Biotech).

Genetic analysis

Fragments surrounding the reported FATP4 exon 3 G/A (Gly209Ser) and intron 11 G/A polymorphisms and a fragment surrounding a novel intron 11 4T/3T polymorphism that was detected by sequencing were PCR amplified for subsequent analysis by pyrosequencing (16). For the exon 3 polymorphism, fragments were amplified as above using 6 pmol of each primer 5′-biotin-GTGAGGTCCATGCCAGCCTG-3′ and 5′-CACCTGTGAAGCCCTTGTCAG-3′. Fragments surrounding the intron 11 G/A and 4T/3T polymorphisms were amplified with 5 pmol of each primer 5′-biotin-GGCTGTTACTTGACCTCTGCACAC-3′ and 5′-GCGCTGTGCCTGGCACCTAATATG-3′ in 1.5 mM $MgCl_2$ and 5 pmol of each primer 5′-biotin-GGCTGTTACTTGACCTCTGCACAC-3′ and 5′-GCCTCTCTCCTGCTCTAAAACTCC-3′ in 1.75 mM $MgCl_2$, respectively, with 1 U *Taq* DNA polymerase (Promega) using touch-down thermocycling with 20 final cycles of 30-sec steps at 94 C, 56 C, and 72 C. Samples were prepared and analyzed on a PSQ96 instrument using the SNP reagent kit in accordance with the manufacturer's recommendations (Pyrosequencing AB, Uppsala, Sweden), with 15 pmol of pyrosequencing primer (5′-GTGCTTGGAGGCACCGCAC-3′, 5′-CAATGTGTGTCTTCTCTGCCAGCC-3′ and 5′-CTGCTCTAAAACTCCAAGAAGGCAAA-3′ for the exon 3 G/A, intron 11 G/A, and intron 11 4T/3T polymorphisms, respectively). ApoE genotyping was performed using PCR and restriction enzyme digestion (17).

Protein structure modeling

Modeling template protein structures were identified by the threading algorithm 3D-PSSM (18) using the FATP4 cDNA (GenBank accession no. NP_005085) as search query. The final model was derived using Modeller4 (19), in which the 3D-PSSM-derived alignment was adjusted to relieve local energetic stress and to optimize the alignment in regions of low similarity. Results were visualized with the RasMol (20) or MolMol (21) software. A consensus of several methods was used to predict FATP4 membrane topology (PSIPRED, PRED-TMR, HMMTOP, TMHMM, TMBASE, www.hgmp.mrc.ac.uk/GenomeWeb/prot-transmembrane.html) and secondary structure (22), respectively. Sequence conservation within the FATP family was visualized in the structural model by ConSurf (23). Sequence alignments were also performed with the BLAST and ClustalW algorithms.

Statistical analysis

The Statview (SAS Institute Inc., Cary, NC) software was used to perform ANOVA and repeated-measures ANOVA. Fisher's protected least significant difference tests were used for *post hoc* analysis. Skewed data were logarithmically transformed before analysis. Homeostasis model assessment (HOMA) index was calculated as the product of fasting insulin and glucose concentrations divided by 22.5 (24). Linkage disequilibrium calculations were performed with the Associate software 2.35 (J. Ott, Rockefeller University, New York, NY). Statistical significance was assigned to a value of $P < 0.05$.

Results

Prevalence of polymorphisms

In a cohort of 608 healthy 50-yr-old Swedish men, frequencies of the rare alleles were 0.05 for both the FATP4 exon 3 G/A (Gly209Ser) and intron 11 G/A polymorphisms reported in the National Center for Biotechnology Information SNP database (Table 1). Notably, Ser209 is reported as wild-type in murine FATP4 (7, 25). A T/C polymorphism at position −856 in the FATP4 putative proximal promoter region and a C/T polymorphism at position 1542 in exon 10 reported in the NCBI SNP database were not found after direct sequencing of 48 alleles. A novel 4T/3T polymorphism at position 249 in intron 11, identified when screening for the intron 11 G/A polymorphism, exhibited a frequency of 0.10 for the rare 3T allele (Table 1). No obvious impact on any consensus transcription factor binding site was judged to be conveyed by either the intron 11 G/A polymorphism or the intron 11 4T/3T polymorphism (Ref. 26; http://www.cbrc.jp/research/db/TFSEARCH.html). A novel G/A polymorphism at position −908 identified when screening for the −856 T/C polymorphism showed a frequency of only 0.01 for the rare allele and was not observed to significantly alter any consensus transcription factor binding site (Ref. 26; http://www.cbrc.jp/research/db/TFSEARCH.html) and was therefore not investigated further. The Gly209Ser and intron 11 4T/3T polymorphic loci were in strong linkage

TABLE 1. FATP4 genotype and allele frequencies and linkage disequilibrium in the whole cohort of Swedish men and in the OFTT subset

	Gly209Ser						Intron 11 G/A						Intron 11 4T/3T					
	n[a]	Genotype frequencies (n)			Allele frequencies		Linkage diseq.[b]		n[a]	Genotype frequencies (n)			Allele frequencies		Linkage diseq.[b]	n[a]	Genotype frequencies (n)			Allele frequencies	
		Gly/Gly	Gly/Ser	Ser/Ser	Gly	Ser	Intron 11 G/A	Intron 11 4T/3T		G/G	G/A	A/A	G	A	Intron 11 4T/3T		4T/4T	4T/3T	3T/3T	4T	3T
Total																					
	605	553	49	3	0.95	0.05	$D' = -0.66$ $P = 0.44$	$D' = 0.98$ $P < 0.0001$	608	549	54	5	0.95	0.05	$D' = -0.43$ $P = 0.42$	602	490	107	5	0.90	0.10
OFTT																					
	107	98	8	1	0.95	0.05			107	100	7	0	0.97	0.03		105	84	19	2	0.89	0.11

[a] Total number of individuals analyzed vary due to technical reasons.
[b] Linkage disequilibrium (D′) calculated for whole cohort only.

disequilibrium, whereas the intron 11 G/A locus was not in strong linkage disequilibrium with either of the other two loci (Table 1). All genotyping assays gave identical results, compared with those from direct sequencing of a limited number of individuals. Sequencing FATP4 exon 3, codon 194 was found to read CTG (Leu) in all of a total of 88 alleles, in accordance with the GenBank genomic clone AC006312, and not CCG (Pro) as in the GenBank FATP4 mRNA AF055899.

Clinical characteristics

For each of the three polymorphisms, the number of rare homozygotes was low, especially in the OFTT subset, and certain parameters exhibited considerable variability within the rare homozygote groups. Therefore, comparisons of common homozygotes and heterozygotes were focused on (using *post hoc* tests), and little weight was attached to observations regarding rare homozygotes [for example, the high mean insulin concentration in Ser209 homozygotes, which is hard to interpret due to the very small sample size (n = 3) and large variability of this parameter in these individuals; Table 2].

Heterozygotes for the Gly209Ser polymorphism had significantly lower body mass index (BMI) than common homozygotes (Table 2). Systolic blood pressure (SBP), plasma TG, VLDL-TG and insulin concentrations, and HOMA index were also significantly lower in Gly/Ser heterozygotes compared with common homozygotes, as shown by ANOVA and/or *post hoc* analysis, the latter corrected for BMI (Table 2). Diastolic blood pressure tended to be lower in carriers of the Ser209 allele (data not shown).

The phenotypic modulation associated with the intron 11 4T/3T polymorphism was similar to that of the Gly209Ser polymorphism regarding some variables (BMI, SBP, and TG concentrations; Table 2), as expected, due to the almost complete linkage disequilibrium between these two polymorphic loci. However, when analyzing the intron 11 4T/3T polymorphism in Gly209 homozygotes only, BMI was the only variable that remained significantly different between genotypes (4T/4T, 26.2 ± 0.15 kg/m^2; n = 475; 4T/3T, 25.0 ± 0.39; n = 62; $P < 0.01$). Heterozygotes for the intron 11 G/A polymorphism had significantly lower LDL cholesterol concentrations than common homozygotes (Table 2).

In a subset of 107 subjects with the apoE3/E3 genotype who underwent an OFTT allele frequencies were similar to those in the cohort as a whole (Table 1). Plasma TG concentrations at each time point (measured every hour 0–6 h after food intake) tended to be lower in carriers of the rare allele of the Gly209Ser polymorphism (Fig. 1) as well as the intronic polymorphisms (data not shown). Similarly, for all three polymorphisms, heterozygotes exhibited a tendency toward lower NEFA concentrations, chylomicron/chylomicron remnant ($S_f > 400$) apoB48, and VLDL-I (S_f 60–400) and VLDL-II (S_f 20–60) apoB100 concentrations measured at 0, 3, and 6 h after food intake, compared with common homozygotes (data not shown). No significant differences between heterozygotes and common homozygotes in the postprandial lipid or lipoprotein response pattern, as judged by repeated-measures ANOVA, were observed for any of the three polymorphisms.

TABLE 2. BMI, SBP, and fasting metabolic variables according to FATP4 Gly209Ser, intron 11 G/A, and intron 11 4T/3T genotype in healthy, middle-aged Swedish men

	Gly209Ser				Intron 11 G/A				Intron 11 4T/3T			
	Gly/Gly (n = 546)	Gly/Ser (n = 48)	Ser/Ser (n = 3)	*P*	G/G (n = 541)	G/A (n = 53)	A/A (n = 5)	*P*	4T/4T (n = 482)	4T/3T (n = 106)	3T/3T (n = 5)	*P*
BMI (kg/m^2)	26.0 ± 0.14	24.9 ± 0.45[a]	25.6 ± 1.15	0.06	26.0 ± 0.14	25.9 ± 0.42	23.9 ± 1.41	NS	26.1 ± 0.15	25.0 ± 0.30[a]	24.9 ± 0.75	<0.005
SBP (mm Hg)	124.3 ± 0.61	118.6 ± 2.03[a]	119.3 ± 0.67	<0.05	124.0 ± 0.61	123.6 ± 2.39	115.2 ± 5.31	NS	124.9 ± 0.67	120.6 ± 1.28[a]	121.8 ± 5.75	<0.05
Triglycerides (mmol/liter)	1.59 ± 0.04	1.32 ± 0.13[a]	1.07 ± 0.30	<0.05	1.57 ± 0.04	1.57 ± 0.15	1.21 ± 0.34	NS	1.62 ± 0.05	1.31 ± 0.07[a]	1.33 ± 0.44	<0.01
VLDL-TG (mmol/liter)	1.17 ± 0.04	0.92 ± 0.11[a]	0.70 ± 0.27	<0.05	1.15 ± 0.04	1.20 ± 0.14	0.79 ± 0.32	NS	1.20 ± 0.04	0.90 ± 0.06[a]	0.89 ± 0.37	<0.01
Total cholesterol (mmol/liter)	5.38 ± 0.04	5.25 ± 0.15	5.00 ± 0.56	NS	5.40 ± 0.04	5.16 ± 0.12	5.10 ± 0.45	NS	5.39 ± 0.05	5.34 ± 0.10	5.07 ± 0.44	NS
HDL cholesterol (mmol/liter)	1.22 ± 0.01	1.31 ± 0.05	1.45 ± 0.23	NS	1.22 ± 0.01	1.24 ± 0.05	1.45 ± 0.14	NS	1.22 ± 0.02	1.28 ± 0.03	1.42 ± 0.18	NS
LDL cholesterol (mmol/liter)	3.57 ± 0.04	3.54 ± 0.11	3.45 ± 0.44	NS	3.60 ± 0.04	3.34 ± 0.11[a]	2.95 ± 0.28	<0.05	3.56 ± 0.04	3.60 ± 0.09	3.26 ± 0.31	NS
NEFA (mmol/liter)	0.422 ± 0.007	0.413 ± 0.026	0.177 ± 0.072	<0.05	0.42 ± 0.007	0.405 ± 0.027	0.48 ± 0.22	NS	0.423 ± 0.007	0.412 ± 0.018	0.302 ± 0.105	NS[b]
Insulin (pmol/liter)	44.25 ± 1.05	38.47 ± 2.92[a]	71.93 ± 22.72	0.05	44.06 ± 1.04	43.97 ± 3.63	31.92 ± 1.65	NS	44.50 ± 1.12	40.17 ± 2.18	53.96 ± 16.63	NS[b]
Glucose (mmol/liter)	4.98 ± 0.03	4.92 ± 0.09	4.27 ± 0.58	0.06	4.98 ± 0.03	4.94 ± 0.10	5.14 ± 0.23	NS	4.98 ± 0.03	4.95 ± 0.06	4.58 ± 0.38	NS
HOMA	1.67 ± 0.05	1.45 ± 0.14[a]	2.33 ± 0.96	NS	1.66 ± 0.05	1.65 ± 0.15	1.22 ± 0.11	NS	1.68 ± 0.05	1.52 ± 0.10	1.80 ± 0.62	NS[b]

Data ± SEM. Skewed data logarithmically transformed prior to analysis. ANOVA *P* values stated. NS, Not significant.

[a] Significant difference between heterozygotes and common homozygotes according to Fisher's *post hoc* test ($P < 0.05$). Because BMI differed significantly according to Gly209Ser and intron 11 4T/3T genotype, *post hoc* tests were corrected for BMI when analyzing all other variables for these two polymorphisms.

[b] Correction for BMI could not be performed due to significant interaction between genotype and BMI.

FIG. 1. Plasma TG concentrations during an OFTT in healthy 50-yr-old men with the apoE3/E3 genotype, according to FATP4 Gly209Ser genotype. No significant differences according to genotype were observed. Gly/Gly (○; n = 98), Gly/Ser (●; n = 8), Ser/Ser (▲; n = 1). Mean values ± SEM.

Structural evaluation

To investigate structural-functional aspects of FATP4, including potential effects of the Gly209Ser substitution on FATP4 function, a structural model of the FATP4 protein structure was generated. The FATP4 protein was judged to adopt the fold of the adenylate-forming enzyme superfamily because several members of this family were picked up by both BLAST searches of the Protein Data Bank (PDB) and by the threading algorithm 3D-PSSM (18) using the FATP4 sequence as search query. The resultant candidate structural templates identified for FATP4 were the PDB entries 1PG4 (*Salmonella enterica* acetyl-CoA synthase) (seACS) (27), 1MD9 (*Bacillus subtilis* 2,3-dihydroxybenzoate-AMP ligase) (10), and 1BA3 [*Photinus pyralis* luciferase (28), represented by 1LCI (29) in 3D-PSSM]. Despite low overall sequence identities (15–20%), the AMP-binding motif was nearly identical, as were a number of strictly invariant residues within the superfamily of adenylate-forming enzymes (29) (Fig. 2). seACS was chosen as template for modeling of the FATP4 structure because it scored highest, both with respect to sequence similarity and structural conservation (>95% certainty in 3D-PSSM).

The model suggested an overall FATP4 protein structure consisting of a large N-terminal domain and a smaller C-terminal domain. At their interface, the AMP-binding motif was located in a cleft, similarly to its position in the catalytic cleft of the adenylate-forming enzymes (27) (Fig. 3). Catalytic activity of this FATP4 region is suggested because directed mutagenesis of residues within the AMP-binding motif of both FATP1 and the yeast FATP homolog Fat1p was shown to severely impair azido-ATP binding, FA transport, and acyl-CoA synthase activity (9, 11, 12) (Fig. 3). Furthermore, FATP4 residues Asp488 and Arg503, distant in sequence from the AMP-binding motif but folded toward it (Fig. 3), are identical with AMP-binding residues in the active site of adenylate-forming enzymes (Fig. 2) (10, 27). These residues are conserved throughout the FATP family (Fig. 2) and were also shown to be critical for Fat1p acyl-CoA synthase and FA transport activity (12). The entire cleft region between the two domains showed high surface conservation within the

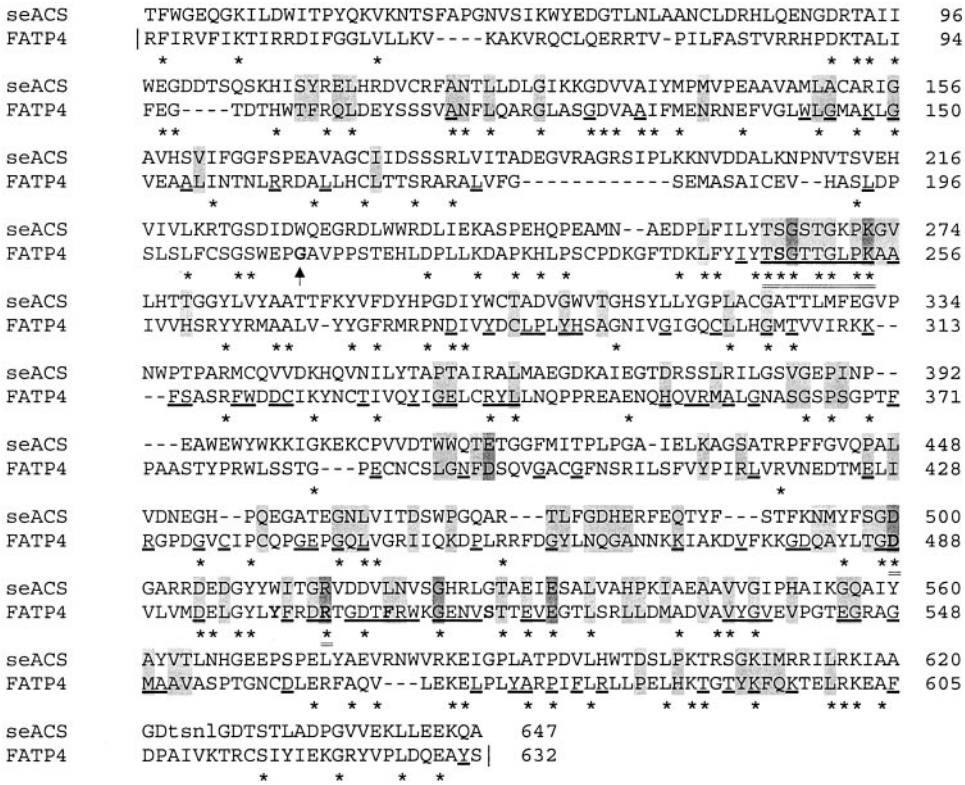

FIG. 2. Alignment of the seACS and FATP4 sequences used for the generation of the FATP4 structural model (PDB entry 1PG4 and GenBank accession no. NP_005085 with Leu194, respectively). The FATP4 residues 1–39 and 633–641 were not conserved in seACS and were therefore omitted from the model (indicated with |). Disordered residues in the 1PG4 structure are in *lowercase letters*. Invariant positions in the alignment are indicated with an *asterisk*. The *boxed* residues represent invariant (*dark gray*) and homologous (>50% identical; *light gray*) positions in an alignment of 38 adenylate-forming enzymes (29). *Underlined* residues represent invariant positions in an alignment of FATP1–6 (GenBank accession nos. CAC07591, NP_003636, NP_077306, NP_005085 with Leu194, NP_036386, NP_054750, respectively). The variable FATP4 residue 209 is in *boldface* and indicated with an *arrow*. The consensus AMP-binding motif is *underlined with a double line*. FATP4 residues corresponding to those shown critical for Fat1p function by directed mutagenesis are indicated (*boldface* and *underlined with a double line*: Ser247 corresponding to Fat1p Ser258, in AMP-binding motif; Asp488 and Arg503 corresponding to Fat1p Asp508 and Arg523, also implicated in AMP binding; *bold-face*: Tyr499, Phe508, Ser516 corresponding to Fat1p Tyr519, Phe528, and Ser536).

FATP family (Fig. 3), indicating its importance for FATP function. Together, these observations suggest a catalytic region that is structurally and functionally conserved between the FATP and adenylate-forming enzyme families.

The FATP4 model revealed a large positively charged surface (Fig. 3), surface-continuous but sequence-discontinuous, indicative of association to a phospholipid-containing membrane. The amino-terminal approximately 40 residues of FATP4 not represented in the model (Fig. 2) were predicted to form a *trans*-membrane helix that could anchor the protein to the membrane (Fig. 3). Thus, the present model is consistent with a cytosolic, membrane-bound protein with an extracellular N terminus, as experimentally shown for FATP1 (30).

The variable residue 209 was located in an exposed loop connecting two β-strands, in a region of the protein predicted to face the cytosol. A Gly-to-Ser mutation could well influence the loop structure due to structural limitations of adoptable backbone angles. Although flanked by sequence stretches similar with seACS, the exposed residues surrounding FATP4 residue 209 exhibited relatively high variability within the FATP family as well as within the structurally conserved adenylate-forming enzyme family (Figs. 2 and 3) (10), suggesting that these residues may convey protein-specific properties. Furthermore, the variable residue 209 was flanked by proline residues (SWEPG/SAVPP), which is typical of short interactive protein segments (31), and other hydrophobic residues. Taken together, this could well indicate that these residues are involved in protein-specific interactions.

Discussion

We found that a G/A polymorphism in exon 3 of the FATP4 gene, giving rise to a Gly209Ser substitution with potential structural-functional implications, is significantly associated with several features of the insulin resistance syndrome. Classically, Syndrome X was defined by Reaven (32) as a clustering of insulin resistance (as manifested by impaired insulin-stimulated glucose uptake, glucose intolerance, and hyperinsulinemia) with increased VLDL-TG concentrations, decreased HDL cholesterol concentrations, and hypertension. In this study, the rare Ser209 allele was significantly associated with lower HOMA index, suggesting an improved insulin sensitivity in carriers of the Ser209 allele (33), and other phenotypes associated with this allele were

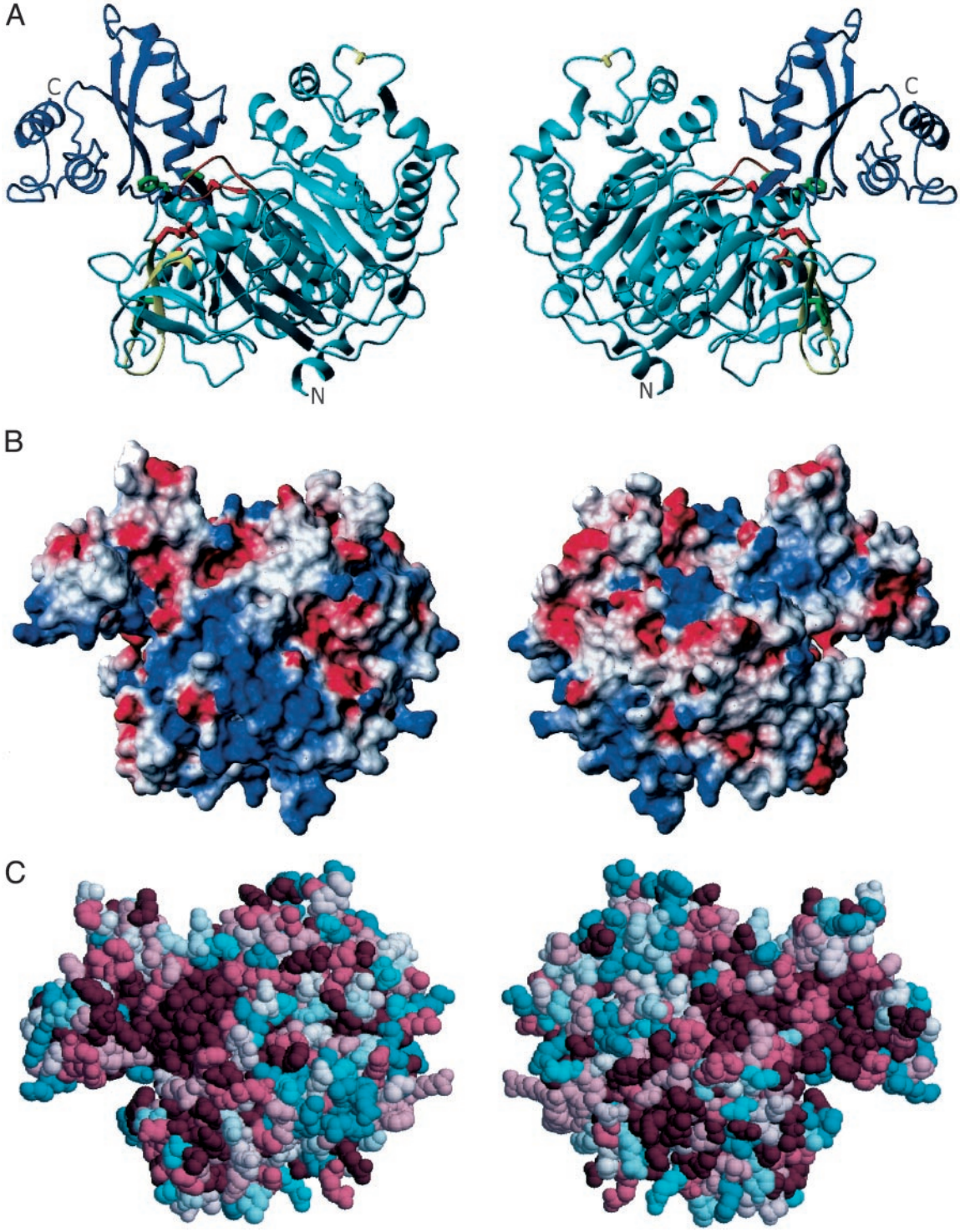

FIG. 3. Presentation of the FATP4 structural model. A–C are in similar orientation, with 180-degree rotation between the *left* and *right* column. A, Ribbon representation. The N-terminal domain is colored in *turquoise*, the C-terminal domain in *blue*. The N-terminal and C-terminal ends of the model are indicated (FATP4 residues 40 and 632, respectively). The variable residue 209 is in ball-and-stick representation and colored in *yellow*. The consensus AMP-binding motif is colored *red*. Residues corresponding to those shown critical for Fat1p function by directed mutagenesis are in ball-and-stick representation and colored in *red* (Ser247 corresponding to Fat1p Ser258; in AMP-binding motif, Asp488 and Arg503 corresponding to Fat1p Asp508 and Arg523; also implicated in AMP-binding) or *green* (Tyr499, Phe508, Ser516 corresponding to Fat1p Tyr519, Phe528, and Ser536). FACS signature motif residues conserved in FATP4 (residues 486–503) are colored in *yellow*. B, Presentation of surface electrostatics. Positively charged residues are shown in *blue*, negative in *red*. The large continuous positive (*blue*) surface (*left column*), also extending slightly to the other side (*right column*), is suggested to be oriented toward a negatively charged membrane surface, with a predicted *trans*-membrane helix protruding from the N terminus of the model. C, Surface conservation within the FATP family by visualization of a ClustalW alignment of FATP1–6 on the FATP4 model. Degree of conservation is color coded according to a gradient from *blue* (variable) over *white* to *red* (conserved).

consistent with improved insulin sensitivity (lower fasting insulin and TG concentrations and lower SBP) independent of significant variations in BMI. Furthermore, carriers of the Ser209 allele exhibited tendencies toward lower fasting NEFA concentrations, reduced measures of postprandial lipemia, and higher HDL cholesterol concentrations (Table 2), also consistent with improved insulin sensitivity.

An intron 11 4T/3T polymorphism exhibited phenotypic associations resembling those of the Gly209Ser polymorphism, and an intron 11 G/A polymorphism was associated with LDL cholesterol concentrations. When analyzing the intron 11 4T/3T polymorphism in Gly209 homozygotes only, most of the significant associations were lost, indicating that the phenotype associated with the intron 11 4T/3T polymorphism was to a large extent dependent on the strong linkage disequilibrium between the intron 11 3T and Ser209 alleles. This is supported by the potential functionality of the Gly209Ser substitution, as indicated by the structural evaluation of this amino acid change and by the fact that there was no clear implication of either of the intronic polymorphisms in differential transcriptional regulation. However, influence of the intronic polymorphisms on co- or posttranscriptional processes cannot be ruled out.

The striking phenotypic differences associated with the Gly209Ser polymorphism may readily be explained by variations in NEFA uptake and metabolism and more specifically by variations in FATP4 activity. NEFA concentrations are strongly related to insulin sensitivity, in that high NEFA concentrations are associated with reduced peripheral insulin-stimulated glucose uptake and increased hepatic glucose output (1). This might be explained by high NEFA concentrations metabolically influencing glucose homeostasis (1, 34), NEFA-mediated transcriptional regulation (35), and physical-chemical effects of NEFAs. The observed variations in both fasting and postprandial TG concentrations could be explained by differences in peripheral TG clearance and/or hepatic VLDL-TG secretion. The relatively more insulin-resistant phenotypes associated with the common Gly209 allele may include impaired insulin-mediated inhibition of VLDL secretion and adipose tissue hormone-sensitive lipase activity, and impaired insulin-stimulated activation of peripheral lipoprotein lipase. Furthermore, high local NEFA concentrations *per se* may impair lipoprotein lipase activity, and high circulating NEFA concentrations may increase hepatic VLDL-TG synthesis and secretion. An insulin resistance-related hypertensive phenotype may be caused by high concentrations of TGs or NEFAs inducing endothelial dysfunction by interfering with endothelial nitric oxide synthase activity (36, 37). FATP4 expression levels in isolated enterocytes are strongly correlated with uptake of long-chain FAs (13), suggesting that the observations in the postprandial test could be explained by differences in gastrointestinal absorption of FAs. However, because the majority of the observations in this study concern fasting variables, we assume that the primary effects associated with the polymorphisms studied also involve tissues other than gastrointestinal, such as adipose tissue, skeletal muscle, or liver.

In the proposed FATP4 structural model, the variable residue 209 was located in an exposed hydrophobic loop structure flanked by proline residues, suggested to convey protein-specific interactive properties. The candidate structural template *B. subtilis* 2,3-dihydroxybenzoate-AMP ligase and several other adenylate-forming enzymes are part of multienzyme complexes (10), indicating that the FATP4 structure also may comprise regions for potential protein-protein interaction. Such interactions could involve cytosolic tissue-specific FA binding proteins (FABPs) (38), acyl-CoA synthases, or CD36, the latter two having been shown to colocalize with FATPs at the plasma membrane (39, 40). Interestingly, residues 191–475 of murine FATP1 have been shown to direct formation of functional FATP1 homodimers (41). Thus, the phenotypic modulation associated with the Gly209Ser substitution might be due to allelic differences in protein-protein interactions required either for the formation of functional FATP4 dimers or for interaction of FATP4 with other proteins involved in cellular FA handling.

The current study suggests a structural and functional classification of FATP4, and thereby other FATPs, as membrane-associated members of the adenylate-forming enzyme superfamily (including acyl-CoA synthases). Despite low overall sequence similarities, functionally critical regions in this superfamily were very similar in FATP4, both at the levels of sequence and structure (Figs. 2 and 3). A substantial amount of experimental data regarding intrinsic FATP acyl-CoA synthase activity, and the importance of the AMP-binding motif for FATP function (9, 11, 12, 25), is in excellent agreement with this classification.

The functionality of the proposed FATP4 catalytic cleft is supported by the fact that conserved residues, implicated in AMP binding in FATP4 (Figs. 2 and 3), were shown important for azido-ATP binding, acyl-CoA synthase activity, and FA transport activity in FATP1 and the yeast FATP homolog Fat1p by directed mutagenesis (9, 11, 12), as described above. Furthermore, other mutations that severely affected Fat1p function (12) (corresponding to FATP4 Tyr499, Phe508, and Ser516) map to the cleft region (Fig. 3), as does a conserved fatty acyl-CoA synthase (FACS) signature motif proposed to contribute to the FA binding site in the *Escherichia coli* FACS (42, 43) (Fig. 3). Interestingly, certain of the above Fat1p mutations selectively affected either acyl-CoA synthase activity or FA import (12). The proximity of the proposed catalytic region and membrane-binding surface suggests that they might be functionally linked in the context of FA binding. Of note, the interdomain orientation of adenylate-forming enzymes has been proposed to be significantly altered during their two-step catalytic reaction (adenylation and thioesterification by acyl-CoA synthases) (27). This suggests that the interface between the two domains could be important for such a reorientation as a functional feature in FATP-mediated acyl-CoA formation and FA transport.

In summary, we conclude that alterations in NEFA uptake and/or metabolism may underlie the phenotypes observed in this study and that these alterations may be caused by Gly209Ser genotype-associated variations in FATP4 activity in metabolically relevant tissues. Furthermore, we propose a model of FATP4 structure, including identification of regions with specific functionality, that will prove useful in further studies to evaluate the physiological and pathological role(s) of the FATPs.

Acknowledgments

Received April 22, 2003. Accepted September 29, 2003.

Address all correspondence and requests for reprints to: Rachel Fisher, King Gustaf V Research Institute, Karolinska Hospital, S-171 76 Stockholm, Sweden. E-mail: rachel.fisher@medks.ki.se.

This work was supported by grants from the Swedish Medical Research Council (project 8691), the Söderberg Foundation, the Swedish Heart and Lung Foundation, the Swedish Institute, the Swedish National Network and Graduate School for Cardiovascular Research, the Professor Nanna Svartz Foundation, the Åke Wiberg Foundation, the Nilsson-Ehle Foundation, the Fredrik and Ingrid Thuring Foundation, the Gamla Tjänarinnor Foundation, and the Sigurd and Elsa Goljes Foundation.

Present address for M.S.: Molecular Biotechnology, IFM, Linköping University, S-581 83 Linköping, Sweden.

References

1. **Boden G** 1999 Free fatty acids, insulin resistance, and type 2 diabetes mellitus. Proc Assoc Am Physicians 111:241–248
2. **Stremmel W, Strohmeyer G, Borchard F, Kochwa S, Berk PD** 1985 Isolation and partial characterization of a fatty acid binding protein in rat liver plasma membranes. Proc Natl Acad Sci USA 82:4–8
3. **Abumrad NA, el-Maghrabi MR, Amri EZ, Lopez E, Grimaldi PA** 1993 Cloning of a rat adipocyte membrane protein implicated in binding or transport of long-chain fatty acids that is induced during preadipocyte differentiation. Homology with human CD36. J Biol Chem 268:17665–17668
4. **Schaffer JE, Lodish HF** 1994 Expression cloning and characterization of a novel adipocyte long chain fatty acid transport protein. Cell 79:427–436
5. **Ibrahimi A, Bonen A, Blinn WD, Hajri T, Li X, Zhong K, Cameron R, Abumrad NA** 1999 Muscle-specific overexpression of FAT/CD36 enhances fatty acid oxidation by contracting muscle, reduces plasma triglycerides and fatty acids, and increases plasma glucose and insulin. J Biol Chem 274:26761–26766
6. **Febbraio M, Abumrad NA, Hajjar DP, Sharma K, Cheng W, Pearce SF, Silverstein RL** 1999 A null mutation in murine CD36 reveals an important role in fatty acid and lipoprotein metabolism. J Biol Chem 274:19055–19062
7. **Hirsch D, Stahl A, Lodish HF** 1998 A family of fatty acid transporters conserved from mycobacterium to man. Proc Natl Acad Sci USA 95:8625–8629
8. **Fitscher BA, Riedel HD, Young KC, Stremmel W** 1998 Tissue distribution and cDNA cloning of a human fatty acid transport protein (hsFATP4). Biochim Biophys Acta 1443:381–385
9. **Coe NR, Smith AJ, Frohnert BI, Watkins PA, Bernlohr DA** 1999 The fatty acid transport protein (FATP1) is a very long chain acyl-CoA synthetase. J Biol Chem 274:36300–36304
10. **May JJ, Kessler N, Marahiel MA, Stubbs MT** 2002 Crystal structure of DhbE, an archetype for aryl acid activating domains of modular nonribosomal peptide synthetases. Proc Natl Acad Sci USA 99:12120–12125
11. **Stuhlsatz-Krouper SM, Bennett NE, Schaffer JE** 1999 Molecular aspects of fatty acid transport: mutations in the IYTSGTTGXPK motif impair fatty acid transport protein function. Prostaglandins Leukot Essent Fatty Acids 60:285–289
12. **Zou Z, DiRusso CC, Ctrnacta V, Black PN** 2002 Fatty acid transport in *Saccharomyces cerevisiae*. Directed mutagenesis of FAT1 distinguishes the biochemical activities associated with Fat1p. J Biol Chem 277:31062–31071
13. **Stahl A, Hirsch DJ, Gimeno RE, Punreddy S, Ge P, Watson N, Patel S, Kotler M, Raimondi A, Tartaglia LA, Lodish HF** 1999 Identification of the major intestinal fatty acid transport protein. Mol Cell 4:299–308
14. **Gertow K, Skoglund-Andersson C, Eriksson P, Boquist S, Orth-Gomér K, Schenck-Gustafsson K, Hamsten A, Fisher RM** 2003 A common polymorphism in the fatty acid transport protein-1 gene associated with elevated post-prandial lipaemia and alterations in LDL particle size distribution. Atherosclerosis 167:265–273
15. **Boquist S, Ruotolo G, Tang R, Bjorkegren J, Bond MG, de Faire U, Karpe F, Hamsten A** 1999 Alimentary lipemia, postprandial triglyceride-rich lipoproteins, and common carotid intima-media thickness in healthy, middle-aged men. Circulation 100:723–728
16. **Ronaghi M, Karamohamed S, Pettersson B, Uhlen M, Nyren P** 1996 Real-time DNA sequencing using detection of pyrophosphate release. Anal Biochem 242:84–89
17. **van den Maagdenberg AM, de Knijff P, Stalenhoef AF, Gevers Leuven JA, Havekes LM, Frants RR** 1989 Apolipoprotein E*3-Leiden allele results from a partial gene duplication in exon 4. Biochem Biophys Res Commun 165:851–857
18. **Kelley LA, MacCallum RM, Sternberg MJ** 2000 Enhanced genome annotation using structural profiles in the program 3D-PSSM. J Mol Biol 299:499–520
19. **Sali A, Blundell TL** 1993 Comparative protein modelling by satisfaction of spatial restraints. J Mol Biol 234:779–815
20. **Sayle RA, Milner-White EJ** 1995 RASMOL: biomolecular graphics for all. Trends Biochem Sci 20:374
21. **Koradi R, Billeter M, Wuthrich K** 1996 MOLMOL: a program for display and analysis of macromolecular structures. J Mol Graph 14:51–55, 29–32
22. **Combet C, Blanchet C, Geourjon C, Deleage G** 2000 NPS@: network protein sequence analysis. Trends Biochem Sci 25:147–150
23. **Glaser F, Pupko T, Paz I, Bell RE, Bechor-Shental D, Martz E, Ben-Tal N** 2003 ConSurf: identification of functional regions in proteins by surface-mapping of phylogenetic information. Bioinformatics 19:163–164
24. **Matthews DR, Hosker JP, Rudenski AS, Naylor BA, Treacher DF, Turner RC** 1985 Homeostasis model assessment: insulin resistance and beta-cell function from fasting plasma glucose and insulin concentrations in man. Diabetologia 28:412–419
25. **Herrmann T, Buchkremer F, Gosch I, Hall AM, Bernlohr DA, Stremmel W** 2001 Mouse fatty acid transport protein 4 (FATP4): characterization of the gene and functional assessment as a very long chain acyl-CoA synthetase. Gene 270:31–40
26. **Heinemeyer T, Wingender E, Reuter I, Hermjakob H, Kel AE, Kel OV, Ignatieva EV, Ananko EA, Podkolodnaya OA, Kolpakov FA, Podkolodny NL, Kolchanov NA** 1998 Databases on transcriptional regulation: TRANSFAC, TRRD and COMPEL. Nucleic Acids Res 26:362–367
27. **Gulick AM, Starai VJ, Horswill AR, Homick KM, Escalante-Semerena JC** 2003 The 1.75 A crystal structure of acetyl-CoA synthetase bound to adenosine-5′-propylphosphate and coenzyme A. Biochemistry 42:2866–2873
28. **Franks NP, Jenkins A, Conti E, Lieb WR, Brick P** 1998 Structural basis for the inhibition of firefly luciferase by a general anesthetic. Biophys J 75:2205–2211
29. **Conti E, Franks NP, Brick P** 1996 Crystal structure of firefly luciferase throws light on a superfamily of adenylate-forming enzymes. Structure 4:287–298
30. **Lewis SE, Listenberger LL, Ory DS, Schaffer JE** 2001 Membrane topology of the murine fatty acid transport protein 1. J Biol Chem 276:37042–37050
31. **Kini RM, Evans HJ** 1996 Prediction of potential protein-protein interaction sites from amino acid sequence. Identification of a fibrin polymerization site. FEBS Lett 385:81–86
32. **Reaven GM** 1988 Banting lecture 1988. Role of insulin resistance in human disease. Diabetes 37:1595–1607
33. **Radziuk J** 2000 Insulin sensitivity and its measurement: structural commonalities among the methods. J Clin Endocrinol Metab 85:4426–4433
34. **Randle PJ, Garland PB, Newsholme EA, Hales CN** 1965 The glucose fatty acid cycle in obesity and maturity onset diabetes mellitus. Ann NY Acad Sci 131:324–333
35. **Long SD, Pekala PH** 1996 Regulation of GLUT4 gene expression by arachidonic acid. Evidence for multiple pathways, one of which requires oxidation to prostaglandin E2. J Biol Chem 271:1138–1144
36. **Lundman P, Eriksson M, Schenck-Gustafsson K, Karpe F, Tornvall P** 1997 Transient triglyceridemia decreases vascular reactivity in young, healthy men without risk factors for coronary heart disease. Circulation 96:3266–3268
37. **Steinberg HO, Tarshoby M, Monestel R, Hook G, Cronin J, Johnson A, Bayazeed B, Baron AD** 1997 Elevated circulating free fatty acid levels impair endothelium-dependent vasodilation. J Clin Invest 100:1230–1239
38. **Coe NR, Bernlohr DA** 1998 Physiological properties and functions of intracellular fatty acid-binding proteins. Biochim Biophys Acta 1391:287–306
39. **Gargiulo CE, Stuhlsatz-Krouper SM, Schaffer JE** 1999 Localization of adipocyte long-chain fatty acyl-CoA synthetase at the plasma membrane. J Lipid Res 40:881–892
40. **Gimeno RE, Ortegon AM, Patel S, Punreddy S, Ge P, Sun Y, Lodish HF, Stahl A** 2003 Characterization of a heart-specific fatty acid transport protein. J Biol Chem 278:16039–16044
41. **Richards MR, Listenberger LL, Kelly AA, Lewis SE, Ory DS, Schaffer JE** 2003 Oligomerization of the murine fatty acid transport protein 1. J Biol Chem 278:10477–10483
42. **Black PN, Zhang Q, Weimar JD, DiRusso CC** 1997 Mutational analysis of a fatty acyl-coenzyme A synthetase signature motif identifies seven amino acid residues that modulate fatty acid substrate specificity. J Biol Chem 272:4896–4903
43. **Black PN, DiRusso CC, Sherin D, MacColl R, Knudsen J, Weimar JD** 2000 Affinity labeling fatty acyl-CoA synthetase with 9-p-azidophenoxy nonanoic acid and the identification of the fatty acid-binding site. J Biol Chem 275:38547–38553